

# In-plane reorientation of magnetization in epitaxial exchange biased Fe/MnPd bilayers

Qing-feng Zhan and Kannan M. Krishnan<sup>a)</sup>

Department of Materials Science, University of Washington, Seattle, Washington 98195, USA

(Received 10 February 2010; accepted 26 February 2010; published online 18 March 2010)

We investigated the in-plane reorientation of magnetization in epitaxial Fe/MnPd bilayers. The samples with various thicknesses of MnPd and Fe layers present a conventional square and an unusual two-step exchange biased hysteresis loops at different temperature. The shape of the loops is reproduced using the coherent rotation model and including the relative orientation of the uniaxial anisotropy with respect to the exchange bias. The parallel and perpendicular uniaxial anisotropies in the ferromagnetic layer are linked to the aligned and the reoriented states, respectively. The magnetic reorientation between the aligned and the reoriented states, which is determined by the competition between the interface exchange coupling and the intrinsic uniaxial energies, is shown to be driven by the temperature, as well as the thickness of MnPd and Fe layers. © 2010 American Institute of Physics. [doi:10.1063/1.3367705]

The exchange bias (EB) effect, observed for a ferromagnet (FM) in contact with a variety of antiferromagnets (AFM), has attracted much interest for decades, in particular, due to the renewed interest in exchange biased bilayers for application in magnetoresistive sensors.<sup>1</sup> The key factor for EB in FM-AFM bilayers is the interface exchange coupling which contributes to both enhancing the coercivity,  $H_c$ , and shifting the hysteresis curve,  $H_{eb}$ . Previous models used to account for the EB effect usually assume an uncompensated AFM surface and a collinear FM-AFM exchange coupling at the interface.<sup>2</sup> However, micromagnetic calculations show that due to the spin-flop coupling the ground state for a compensated FM-AFM interface is an orthogonal magnetic orientation of the FM and AFM spins.<sup>3</sup> The perpendicular exchange coupling can exert an in-plane uniaxial magnetic anisotropy  $K_{sf}$  on the FM layer<sup>4</sup> and has been observed in both compensated and uncompensated FM-AFM coupled bilayers.<sup>5,6</sup> Including the intrinsic uniaxial anisotropy,  $K_{FM}$ , of the FM layers, which may have various origins,<sup>7</sup> the FM magnetic direction is determined by the combined uniaxial anisotropy  $K_u$  resulting from the competition between  $K_{FM}$  and  $K_{sf}$ . Depending on the relative orientation of the two anisotropies, the strength of  $K_u$  is either enhanced or reduced. If  $K_{FM}$  and  $K_{sf}$  favor different directions, an in-plane reorientation of magnetization is theoretically predicted to take place due to the different behavior of the competing anisotropies on the temperature, the film thickness, and the strength of exchange coupling.<sup>8–11</sup>

In this work, we experimentally observed a variety of in-plane magnetic reorientations in Fe/MnPd bilayers with various thicknesses of both FM and AFM layers. The magnetic reorientation occurs between an aligned state (AS) and a reoriented state (RS) which produce the conventional square and the unusual stepped EB loops, respectively. We assume that the intrinsic uniaxial anisotropies of both FM and AFM layers are parallel, thus when the perpendicular coupling is weak, AS has the spins for both FM and AFM collinear to the intrinsic easy axes [Fig. 1(a)]. If the spin-flop

coupling becomes dominant then the spin configuration is reoriented to the RS in which case the moments of FM are aligned perpendicular to their easy axis and the AFM sublattices; moreover, the AFM spins near the interface are slightly canted to lower the interface exchange energy [Fig. 1(b)].

Fe/MnPd bilayers, with the thicknesses for Fe,  $t_{Fe}$ , fixed at 10 nm and for MnPd,  $t_{MnPd}$ , varying from 5 to 75 nm, were deposited on MgO(001) substrates in an Ion Beam Sputtering system.<sup>12</sup> The substrates were annealed at 500 °C for 1 h and held at 120 °C during deposition. All samples were grown in the presence of an in-plane magnetic field,  $H_{growth}=300$  Oe, along the Fe[100] direction and subjected to a subsequent annealing at 230 °C for 1 h in vacuum. A 2 nm protective Pt layer was deposited on top of the films.

The samples was verified by x-ray diffraction (XRD), which confirms the films are epitaxially grown on the substrates with (001) growth orientation for Fe layers and  $a$ -axis normal orientation for MnPd layers [Fig. 2(a)]. The results calculated from XRD indicate that with increasing  $t_{MnPd}$  the normal oriented  $a$ -axis of MnPd is expanded from 3.92 to 4.00 Å, while the lattice constant of Fe is kept at 2.88 Å [Fig. 2(b)]. The expansion of MnPd lattice indicates that the strain caused by the crystal lattice distortion in epitaxial MnPd layers is gradually relaxed via the formation of dislocation with

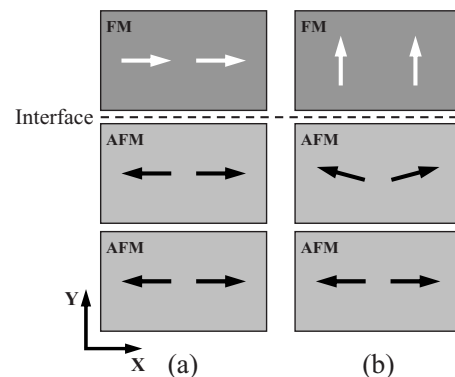


FIG. 1. Schematic of the spin configuration in the interface plane of FM-AFM bilayers in (a) aligned state and (b) reoriented state. The intrinsic uniaxial anisotropies of both FM and AFM subsystems are along  $x$  axis.

<sup>a)</sup>Author to whom correspondence should be addressed. Electronic mail: kannanmk@u.washington.edu.

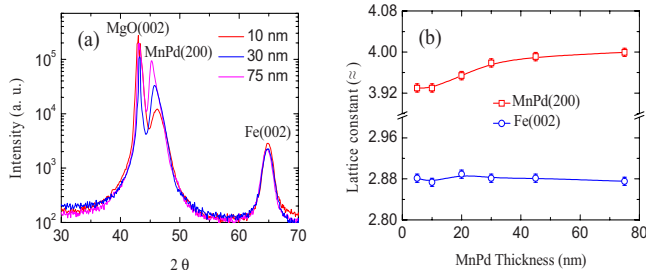


FIG. 2. (Color online) (a) Typical XRD scans for a series of  $a$ -axis oriented Fe(10 nm)/MnPd bilayers with various  $t_{\text{MnPd}}$ . (b) MnPd thickness dependence of lattice constants for Fe and MnPd layers.

increasing  $t_{\text{MnPd}}$ . These dislocations and the boundary between the variants can then give rise to the AFM domain formation.<sup>13,14</sup>

The magnetic properties were characterized using a Quantum Design physical properties measurement system. The samples were cooled from 300 to 10 K under a cooling field,  $H_{\text{cooling}}$ , of 5 KOe parallel to  $H_{\text{growth}}$ . The magnetic field was cycled ten times to minimize the training effect. Subsequently, the hysteresis loops were measured from 10 to 300 K. The bilayers with  $t_{\text{MnPd}} \leq 20$  nm show square loops for the whole range of temperature [Fig. 3(a)]. However, the samples with  $t_{\text{MnPd}} \geq 30$  nm exhibit at low temperature unusual two-step EB loops, in which  $H_1$ ,  $H_2$ ,  $H_3$ , and  $H_4$  are defined as the switching fields for different steps [Fig. 3(b)]. With increasing temperature, the loop shift is decreased and the stepped loop becomes square. The square and stepped loops indicate that the Fe layer has  $K_u$ , which is superimposed on the cubic anisotropy  $K_1$  of Fe, collinear and perpendicular to the applied field  $H$ , respectively.<sup>15</sup>

Although  $H$  aligned with the easy axis often leads to a magnetization reversal by domain nucleation,<sup>16</sup> a coherent rotation model of magnetization can still give us an understanding on how the shape of loops is affected by the relative orientation between  $K_u$  and the EB induced unidirectional anisotropy  $K_{eb}$ .<sup>17,18</sup> The energy per unit volume for the Fe layer with  $H$  applied along  $K_{eb}$  can be expressed as  $E = (K_1/4)\sin^2 2\theta \pm K_u \cos^2 \theta - K_{eb} \cos \theta - M_s H \cos \theta$ , where  $\theta$

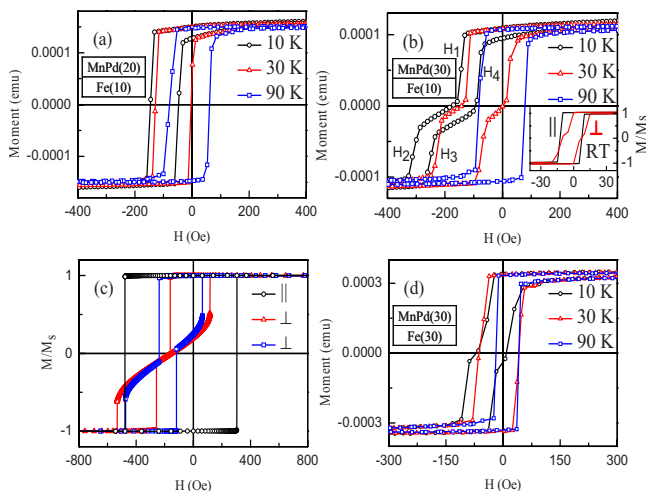


FIG. 3. (Color online) Representative hysteresis loops at various temperature for (a) Fe(10 nm)/MnPd(20 nm), (b) Fe(10 nm)/MnPd(30 nm), and (d) Fe(30 nm)/MnPd(30 nm) bilayers. In the inset of (b), we present the loops obtained at 300 K with the applied field parallel ( $\parallel$ ) and perpendicular ( $\perp$ ) to  $H_{\text{growth}}$ . (c) Calculated hysteresis curves for  $K_u$  parallel ( $\parallel$ ) and perpendicular ( $\perp$ ) to  $K_{eb}$ . The triangles (squares) correspond to a large (small)  $K_u$ .

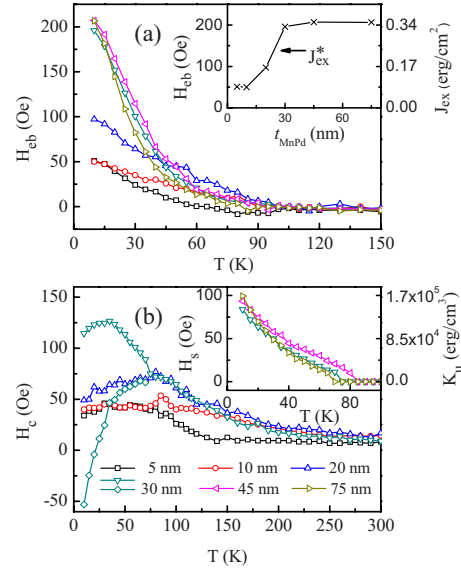


FIG. 4. (Color online) Temperature dependence of (a)  $H_c$  and (b)  $H_{eb}$  for Fe(10 nm)/MnPd bilayers with various  $t_{\text{MnPd}}$ . Inset of (a) shows  $H_{eb}$  and  $J_{ex}$  as a function of  $t_{\text{MnPd}}$  at 10 K. Inset of (b) presents  $H_s$  and  $K_u$  calculated from the stepped EB loops for  $t_{\text{MnPd}} \geq 30$  nm.

is the angle between the magnetization  $M_s$  and  $K_{eb}$ . The sign of the uniaxial term represents the orientation of  $K_u$ . As illustrated in Fig. 3(c), for the AS, where  $K_u \parallel K_{eb}$ , a negative-shifted square loop is obtained with a substantially enhanced coercivity. For the RS i.e.,  $K_u \perp K_{eb}$ , a stepped EB loops can be achieved. Depending on the strength of  $K_u$ ,  $H_1$  can be on the left (squares) or the right (triangles) side of  $H_3$  for small and large value of  $K_u$ , respectively; this is in agreement with the experimental observation in Fig. 3(b).

The switching fields of the square loops,  $H_{\text{left}}$  for the descending and  $H_{\text{right}}$  for the ascending branch, are used to estimate  $H_{eb}$  and  $H_c$  according to  $H_{eb} = -(H_{\text{right}} + H_{\text{left}})/2$  and  $H_c = (H_{\text{right}} - H_{\text{left}})/2$ , respectively. For the stepped loops,  $H_1$  and  $H_3$ , and  $H_2$  and  $H_4$ , are symmetric about  $H_{eb}$ , respectively, thus  $H_{c1} = (H_4 - H_2)/2$ ,  $H_{c2} = (H_3 - H_1)/2$ , and  $H_{eb} = -(H_3 + H_1)/2 = -(H_4 + H_2)/2$ .  $H_{eb}$  and  $H_c$  for the samples with various  $t_{\text{MnPd}}$  are measured from 10 to 300 K and displayed in Figs. 4(a) and 4(b), respectively. Magnetic behaviors for the samples with  $t_{\text{MnPd}} \geq 30$  are almost identical, thus we only plot the representative coercivities to make Fig. 4(b) clearer.  $H_{eb}$  for all the samples is reduced with increasing temperature and eventually vanish at a blocking temperature of  $T_B = 90$  K. Moreover, as observed in other systems,<sup>19</sup> the temperature dependence of  $H_c$  shows, around  $T_B$ , a small and a broad peak for the bilayers with  $t_{\text{MnPd}} = 10$  and 20 nm, respectively. It is well known that the bulk MnPd alloy with CuAu I structure is antiferromagnetic with a Néel temperature of 540 °C.<sup>20</sup> We ascribe  $T_B$ , far lower than  $T_{\text{Néel}}$ , to reduced long-range chemical ordering in MnPd layers.<sup>21</sup> A weak  $H_{eb}$  below 10 Oe can still be observed at 300 K in such bilayers<sup>22</sup> [inset of Fig. 3(b)]. This is probably due to some local regions in MnPd where the chemical ordering is higher than average. Higher post-annealing temperature can result in higher chemical ordering and considerable  $H_{eb}$  at room temperature.<sup>23</sup> We notice that  $H_c$  of the bilayers is larger than that of pure Fe film even when the temperature is far larger than  $T_B$ , which can be also interpreted by the distribution of the chemical ordering parameter of MnPd.

The strength of  $K_u$ , which is perpendicular to  $K_{eb}$ , can be extracted from the stepped loops by using the shift field,  $H_s = (H_{c1} - H_{c2})/2$ , which is related to  $K_u$  through  $K_u = M_s H_s$ .<sup>24</sup> Unfortunately, the square loop is unsuitable for determining  $K_u$  along  $K_{eb}$  because magnetization reversal takes place by domain nucleation. For the bilayers with  $t_{\text{MnPd}} \geq 30$  nm,  $K_u$  aligned perpendicular to  $K_{eb}$  decreases with increasing temperature [inset of Fig. 4(b)]. The critical temperature for  $K_u$  reoriented from perpendicular to parallel to  $K_{eb}$  is a little below  $T_B$ . All the facts suggest that the interface exchange coupling is decisive to produce the perpendicular  $K_u$  inducing RS. On the other hand, the Fe layer has an intrinsic uniaxial anisotropy  $K_{\text{FM}}$  collinear to  $H_{\text{growth}}$ . The square and the two-step loops are obtained at 300 K for  $H$  applied parallel and perpendicular to  $H_{\text{growth}}$ , respectively [inset of Fig. 3(b)].  $K_{\text{FM}}/M_s$  of magnitude  $\sim 5$  Oe can persist down to 10 K. Therefore, we conclude that the in-plane reorientation of  $K_u$  is the consequence of the competition between  $K_{sf}$  and  $K_{\text{FM}}$ . The spin-flop coupling reorients Fe spins perpendicular to the AFM sublattices,<sup>4</sup> whereas  $K_u$  keeps the magnetization of Fe at the intrinsic uniaxial easy axis. The spin-flop model originates from the intrinsically compensated FM-AFM interfaces,<sup>3,4</sup> but this model still can be extended to uncompensated AFM surface, with average compensation of the interface spins produced by interface roughness, domain formation, etc.<sup>8</sup> It is well known that the chemically ordered  $a$ -axis MnPd surface is spin uncompensated.<sup>20</sup> Herein, the behavior of the average compensated FM-AFM interface is likely caused by the chemical disorder in MnPd rather than the interface roughness. On the other hand, the magnetoelastic effect<sup>5</sup> and any uncompensated moments<sup>23</sup> with orthogonal orientation can also account for  $K_u$  perpendicular to  $H_{\text{cooling}}$ . To verify the possibility, we have measured the samples along both/orthogonal Fe easy directions and obtained stepped EB loops identical to that shown in Fig. 3(b). Therefore, for this model to be applicable, the cooling field should align the uncompensated AFM moments orthogonal to it, i.e., a physically unlikely possibility. Moreover, it would be difficult to interpret both  $K_u$  and  $K_{eb}$  along  $H_{\text{cooling}}$ , i.e., the square loops in Fig. 3(a), using such perpendicular moments. Therefore, these two potential mechanisms can be excluded. It should be reiterated that the spin-flop coupling only gives rise to a uniaxial anisotropy but the defect-induced AFM domains lead to a bias.<sup>4,14</sup>

As discussed above, the temperature-driven reorientation of magnetization is observed for the bilayers with  $t_{\text{MnPd}} \geq 30$  nm. From another view of point, the series of samples also shows the AFM thickness-driven magnetic reorientation. At a given temperature, such as 10 K, the samples show a square loop for  $t_{\text{MnPd}} \leq 20$  nm and a stepped EB loop for  $t_{\text{MnPd}} \geq 30$  nm. Both  $t_{\text{Fe}}$  and  $K_{\text{FM}}$  are kept constant for various samples, so the reorientation from AS to RS is due to the enhancement of the spin-flop coupling  $J_{ex}$ , which is related to  $K_{sf}$  through  $K_{sf} \propto -(J_{ex})^2/|J_{\text{AFM}}|$ , where  $J_{\text{AFM}}$  is the exchange coupling in AFM.<sup>9</sup> When  $K_{sf}$  is weak,  $K_{\text{FM}}$  becomes dominant and keeps the Fe spins aligned parallel to  $H_{\text{growth}}$ . If the spin-flop coupling energy is large enough to compensate the increase of both the anisotropy energy of Fe and the intrinsic exchange energy of MnPd,  $K_{sf}$  forces the magnetization of Fe to preferentially reorient perpendicular to the intrinsic Fe uniaxial easy axis.<sup>10</sup> Using the relation  $J_{ex}$

$= H_{eb} t_{\text{Fe}} M_s$  and  $M_s = 1700$  emu/cm<sup>3</sup>,  $J_{ex}$  can be obtained. Following the general trend for the dependence of  $H_{eb}$  on the AFM thickness,<sup>19</sup> at 10 K both  $H_{eb}$  and  $J_{ex}$  for the series of bilayers with fixed  $t_{\text{Fe}}$  are enhanced with increasing  $t_{\text{MnPd}}$  and reach saturation around  $t_{\text{MnPd}} = 30$  nm [inset of Fig. 4(a)]. According to the domain state model, the dislocation created by the lattice relaxation is also a possible reason for the increase of  $H_{eb}$ .<sup>13</sup> The critical value of  $J_{ex}^*$  is estimated to be 0.25 erg/cm<sup>2</sup> to realize the reorientation of magnetization.

The uniaxial anisotropy energy of the FM layer is proportional to its thickness. Therefore, if we keep  $K_{sf}$  unchanged and increase  $t_{\text{Fe}}$ , the enhancement of the uniaxial anisotropy energy of the Fe layer can switch RS back to AS. In order to verify this principle, MnPd(30 nm)/Fe(30 nm) bilayer was made, and the representative loops are shown in Fig. 3(d). At 10 K, this sample shows a stepped loop with a small  $H_{eb}$  and a weak  $K_{sf}$ , as compared to the MnPd(30 nm)/Fe(10 nm) bilayer. Since  $J_{ex}$  as well as  $K_{sf}$  are reduced with increasing temperature,  $K_{\text{FM}}$  becomes dominant at 30 K, and then AS is achieved. Comparing the two samples with the same  $t_{\text{MnPd}}$  but different  $t_{\text{Fe}}$ , the FM thickness-driven magnetic reorientation from RS to AS takes place at 30 K with increasing  $t_{\text{Fe}}$  from 10 to 30 nm while keeping  $t_{\text{MnPd}} = 30$  nm.

This work was supported by DoE/BES under Grant No. ER45987.

<sup>1</sup>J. Nogués and I. K. Schuller, *J. Magn. Magn. Mater.* **192**, 203 (1999).

<sup>2</sup>M. Kiwi, *J. Magn. Magn. Mater.* **234**, 584 (2001).

<sup>3</sup>N. C. Koon, *Phys. Rev. Lett.* **78**, 4865 (1997).

<sup>4</sup>T. C. Schulthess and W. H. Butler, *Phys. Rev. Lett.* **81**, 4516 (1998).

<sup>5</sup>T. J. Moran, J. Nogués, D. Lederman, and I. K. Schuller, *Appl. Phys. Lett.* **72**, 617 (1998).

<sup>6</sup>M. R. Fitzsimmons, C. Leighton, J. Nogués, A. Hoffmann, K. Liu, C. F. Majkrzak, J. A. Dura, J. R. Groves, R. W. Springer, P. N. Arendt, V. Leiner, H. Lauter, and I. K. Schuller, *Phys. Rev. B* **65**, 134436 (2002).

<sup>7</sup>Q. F. Zhan, S. Vandezande, K. Temst, and C. Van Haesendonck, *New J. Phys.* **11**, 063003 (2009).

<sup>8</sup>F. I. F. Nascimento, A. L. Dantas, L. L. Oliveira, V. D. Mello, R. E. Camley, and A. S. Carriço, *Phys. Rev. B* **80**, 144407 (2009).

<sup>9</sup>P. J. Jensen and H. Dreyssé, *Phys. Rev. B* **66**, 220407(R) (2002).

<sup>10</sup>M. L. Silva, A. L. Dantas, and A. S. Carriço, *J. Magn. Magn. Mater.* **292**, 453 (2005).

<sup>11</sup>J. H. Seok, H. Y. Kwon, S. S. Hong, Y. Z. Wu, Z. Q. Qiu, and C. Won, *Phys. Rev. B* **80**, 174407 (2009).

<sup>12</sup>P. Blomqvist, K. M. Krishnan, and D. E. McCready, *J. Appl. Phys.* **95**, 8019 (2004).

<sup>13</sup>U. Nowak, K. D. Usadel, J. Keller, P. Miltényi, B. Beschoten, and G. Güntherodt, *Phys. Rev. B* **66**, 014430 (2002).

<sup>14</sup>A. P. Malozemoff, *J. Appl. Phys.* **63**, 3874 (1988).

<sup>15</sup>R. P. Cowburn, S. J. Gray, J. Ferré, J. A. C. Bland, and J. Miltat, *J. Appl. Phys.* **78**, 7210 (1995).

<sup>16</sup>S. G. Wang, A. Kohn, C. Wang, A. K. Petford-Long, S. Lee, R. Fan, J. P. Goff, L. J. Singh, Z. H. Barber, and R. C. C. Ward, *J. Phys. D* **42**, 225001 (2009).

<sup>17</sup>Y. J. Tang, X. Zhou, X. Chen, B. Q. Liang, and W. S. Zhan, *J. Appl. Phys.* **88**, 2054 (2000).

<sup>18</sup>P. Blomqvist, K. M. Krishnan, and E. Girt, *J. Appl. Phys.* **95**, 8487 (2004).

<sup>19</sup>M. Ali, C. H. Marrows, M. Al-Jawad, B. J. Hickey, A. Misra, U. Nowak, and K. D. Usadel, *Phys. Rev. B* **68**, 214420 (2003).

<sup>20</sup>L. Pál, E. Krén, G. Kádár, P. Szabó, and T. Tarnóczy, *J. Appl. Phys.* **39**, 538 (1968).

<sup>21</sup>M. F. Toney, M. G. Samant, T. Lin, and D. Mauri, *Appl. Phys. Lett.* **81**, 4565 (2002).

<sup>22</sup>N. Cheng, J. Ahn, and K. M. Krishnan, *J. Appl. Phys.* **89**, 6597 (2001).

<sup>23</sup>S. Brück, G. Schütz, E. Goering, X. S. Ji, and K. M. Krishnan, *Phys. Rev. Lett.* **101**, 126402 (2008).

<sup>24</sup>R. Moroni, D. Sekiba, F. B. de Mongeot, G. Gonella, C. Boragno, L. Matterna, and U. Valbusa, *Phys. Rev. Lett.* **91**, 167207 (2003).